

High-Speed Visualization of Temperature Fluctuation in Multiphase AC Arc

H. Maruyama¹, M. Tanaka¹, T. Watanabe¹, H. Nagai², T. Koiwasaki² and T. Okuma^{1,2}

¹Department of Chemical Engineering, Kyushu University, 744 Motoooka, Nishi-ku, Fukuoka 819-0395, Japan

²Panasonic Corporation., 2-7 Matsuba-cho, Kadoma, Osaka 571-8502, Japan

Abstract: Arc fluctuation phenomena and temperature field of a multiphase AC arc were successfully visualized by a high-speed camera with appropriate band-pass filters. The arc temperature was fluctuated up to 13000 K. The high-speed visualization and quantitative analysis of arc swing revealed that the arc was widely distributed because of the arc swing motion due to rotating electromagnetic field. Obtained understandings about arc fluctuation and temperature field will make a practical use of multiphase AC arc to industrial applications.

Keywords: Thermal plasma, high-speed visualization, temperature measurement

1. Introduction

Thermal plasmas have been applied in various industrial fields due to its unique advantages such as high temperature, high enthalpy, and rapid quenching capability. These advantages enable to advance in plasma chemistry and plasma processing [1].

A multiphase AC arc is one of the most attractive thermal plasmas among various thermal plasma reactors because it has many advantages such as high energy efficiency, large plasma volume, low gas velocity, and low equipment cost. Therefore, the multiphase AC arc has been applied to a massive powder processing such as in-flight glass melting [2] and nanomaterial fabrication processes. However, temperature fields and its fluctuation characteristics in the multiphase AC arc have not been understood yet because of the difficulties of temperature measurement in the multiphase AC arc. Understanding the temperature characteristics is significantly necessary to apply the multiphase AC arc to the nanoparticle process and the material synthesis efficiently.

Temperature measurement of thermal plasmas have been conducted to investigate plasma characteristics. Conventionally, optical spectroscopic techniques were widely used to measure the temperature distribution of thermal plasmas. From the spectroscopic data, one dimensional plasma temperature can be determined by several methods, such as the Fowler-Milne method [3], and the Boltzmann plot method [4]. However, spatially resolved profiles of emission intensities from atomic or ionic species should be captured to obtain the spatial distributions of temperature in thermal plasmas. Temperature distributions in radial or axial direction were reported [5]. Recently, the imaging technique based on high-speed camera observation with band-pass filters has been developed. Temperature distribution of free-burning arc was successfully visualized [6].

The purpose of this study is to clarify the arc fluctuation phenomena and temperature fluctuation characteristics of multiphase AC arc. The effect of AC applied condition on the arc fluctuation phenomena and the temperature fluctuation characteristics was discussed because AC

applied condition is one of the most essential parameters to control the plasma field.

2. Temperature Measurement Principle

Visualization of temperature field in multiphase AC was carried out. Conventionally, observation of particular emission from thermal plasma was difficult because many radiations exist around thermal plasma region. Emission from thermal plasma consists of line spectra due to electron transition in the plasma, and continuous spectra due to radiation from the electrode and the reactor wall. In order to measure the temperature, only the line spectra should be extracted. To separate the particular emission from others, an optical system including the band-pass filters was combined with the high-speed camera as shown in **Fig. 1**. The emission from the arc are split into two light paths by the splitter. Two-dimensional emission intensity distributions at each wavelength can be observed on the CCD by using the band-pass filters which transmit different wavelengths.

The temperature measurement was conducted on the basis of Boltzmann plot method. The obtained emission intensity I_{pq} can be expressed as:

$$I_{pq} = \frac{A_{pq}g_p}{\lambda} \cdot \frac{hcN(T)}{4\pi Z(T)} \exp\left(-\frac{E_p}{k_B T}\right) \quad (1)$$

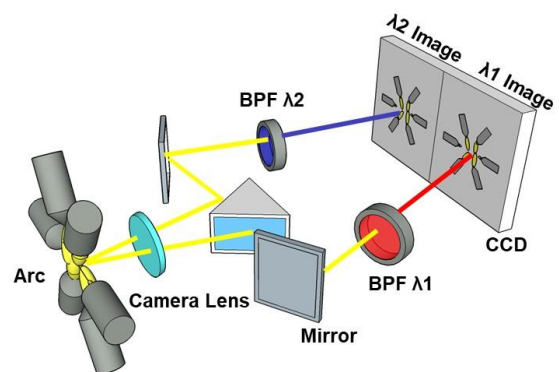


Fig. 1. Schematic diagram of observation system with high-speed camera and band-pass filters.

where A_{pq} is the transition probability, g_p is the statistical weight, h is Planck's constant, c is speed of light, $N(T)$ is a number density of atomic argon at the temperature of T , λ is selected wavelength through band-pass filter, $Z(T)$ is the partition functions, E_p is excitation energy at excited level of p , k_B is the Boltzmann constant, and T is a excitation temperature.

By using Equation (1), the ratio of emission intensities at different wavelengths can be expressed as:

$$\frac{I_{pq}}{I_{p'q'}} = \frac{A_{pq}g_p\lambda_{p'q'}}{A_{p'q'}g_{p'}\lambda_{pq}} \exp\left(-\frac{E_p}{k_B T}\right) \quad (2)$$

The intensity ratio can be expressed as a function of excitation temperature T as:

$$\ln\left(\frac{I_{pq}}{I_{p'q'}} \cdot \frac{A_{p'q'}g_{p'}\lambda_{pq}}{A_{pq}g_p\lambda_{p'q'}}\right) = -\frac{1}{T} \cdot \left(\frac{E_{p'} - E_p}{k_B}\right) \quad (3)$$

The temperature can be calculated from the slope of the graph plotting the term of energy and the term of intensity ratio.

3. Experiments

The schematic diagram of the multiphase AC arcs shown in **Fig. 2**. It consists of 12 electrodes, arc chamber, vacuum pump, and AC power supply at 60Hz. These electrodes with a diameter of 6 mm were made of tungsten (98%) and lanthanum oxide (2wt%). The arc chamber was filled with argon gas. The electrodes are divided into 2 layers consisting of upper and lower 6 electrodes. The upper 6 electrodes are positioned on the horizontal direction, while lower 6 electrodes are at an angle of 30 degree with regard to the horizontal plane. The 12 electrodes are symmetrically arranged by the angle of 30 degree to enlarge the plasma area. The ambient pressure was set at 100 kPa. Arc current for each electrode was fixed at 120A. The distance between the opposing electrodes was 60 nm. Argon gas was injected around each electrode at 2 L/min.

Two kinds of AC applied conditions were compared. One is the case with 12 electrodes and 12-electrically phase. All of the upper and lower electrodes are used and the phase of the AC power supply is set to shift by 30 degree between all 12 electrodes. Another is the case with

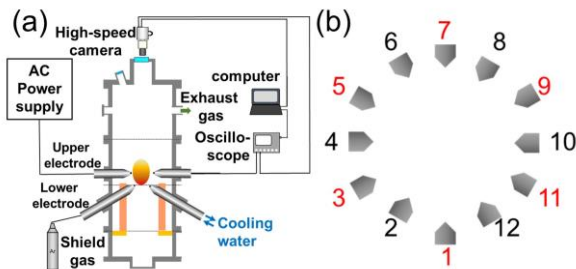


Fig. 2. Schematic image of multiphase AC arc generator (a) and electrode configuration (b).

12 electrodes and 6-electrically phase, called double 6-phase. Voltages of the same phase are supplied to a pair of upper and lower electrodes at the closest distance. The phase of the AC power supply is set to shift by 60 degree between adjacent pair of electrodes.

The observation system consisting of high-speed camera and the band-pass filters was set on top of the chamber. The observation timing was controlled to be synchronized with the trigger signal from the oscilloscope connected to the AC power supply. The band-pass filters of 675 ± 5 nm and 794 ± 5 nm, which include line emissions from atomic argon at 675.2834 nm and 794.8176 nm respectively are used.

4. Results and Discussion

Figure 3 shows high speed camera snapshots of the 12-phase AC arc during one AC cycle and the corresponding arc temperature distributions estimated by Boltzmann plot. These high-speed snapshots were observed through the band-pass filter at 794 nm. Arc fluctuation and corresponding arc temperature in millisecond time scale were visualized by using high-speed camera system. The arc rotated due to the rotating electromagnetic field. These arc discharge leads to arc swing motion. Repetition of arc ignition and extinguishment was observed at all electrodes. This phenomenon is a feature of multiphase AC arc.

The obtained temperature distributions indicated that the temperature of the multiphase AC arc were fluctuated in the range of 7000 K to 13000 K. The arc temperature near the electrode was more than 10000 K. Temperature in the multiphase AC arc is sufficiently high to melt or evaporate refractory metals or ceramics.

Figure 4 shows high speed camera snapshots of the double 6-phase AC arc during one AC cycle and the corresponding arc temperature distributions estimated by Boltzmann plot.

The arc moved at the same time two by two according to applied voltage control. Temperature distribution was 7,000 to 12,000 K, and high temperature of 13,000 K was observed in the vicinity of the electrode. The temperature range is almost the same under both conditions.

In order to clarify the temperature characteristic at the centre of the discharge region, the temperature fluctuations of the central one pixel of the discharge region for different AC applied conditions were measured. The temperature fluctuations in different AC applied conditions are shown in **Fig. 5**. Higher temperature at the centre of the discharge region was often observed at 12-phase than double 6-phase. A high temperature of 7000-10000 K was always observed at 12-phase. In contrast, the arc temperature was always less than the measurement limitation of 7000 K at double 6-phase. This is caused by no existence at the centre of the discharge region.

The arc existence probabilities for different AC applied conditions are shown in **Fig. 6**. The existence probability was defined as the ratio of the time during which the arc existed to total time period of AC cycle. The arc exists widely, and the arc always exists in the centre of the

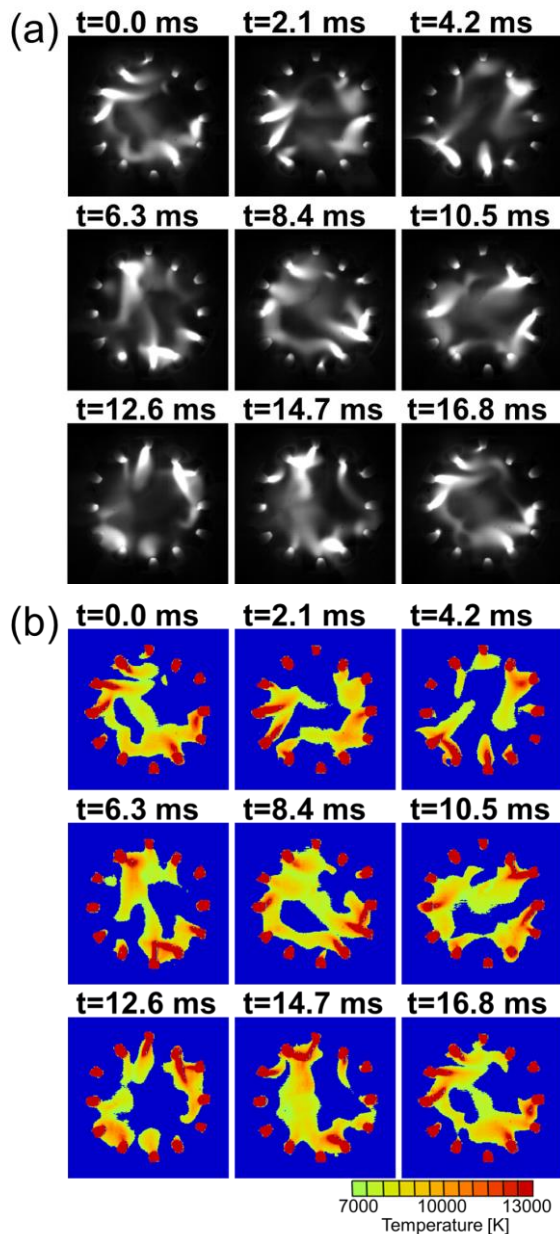


Fig. 3. High-speed snapshots of the multiphase AC arc at 12-phase (a) and corresponding temperature distributions (b).

discharge region at 12-phase. In contrast, the arc exists at a high probability like a donut shape and hardly exist in the centre of the discharge region at double 6-phase. This is due to the difference in the interaction between adjacent arcs. In the double 6-phase, a pair of arcs next to each other in the same phase are controlled by attracting forces due to the influence of the magnetic field generated by arcs. Therefore, the arc discharge is almost similar to the case of 6-phase. Since the adjacent electrode is nearer than the case of 6-phase, arc is easier to discharge to the adjacent electrode. These electrode configurations are the main reasons for arcs to exist like a donut shape.

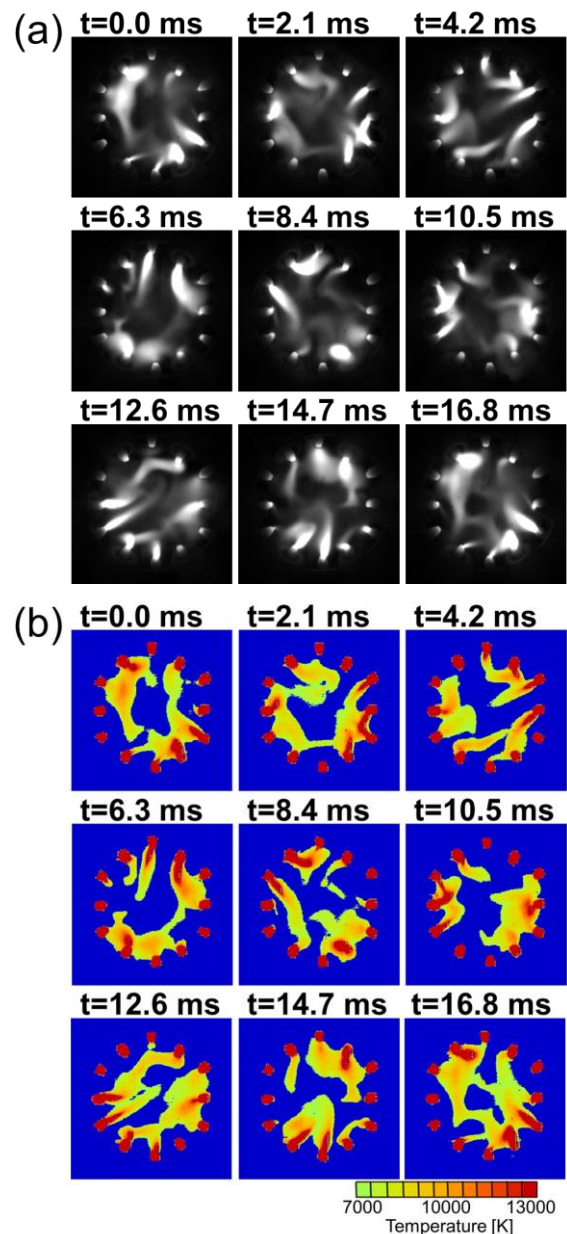


Fig. 4. High-speed snapshots of the multiphase AC arc at double 6-phase (a) and corresponding temperature distributions (b).

The arc swing angle was estimated from high-speed snapshots to understand arc fluctuation. Arc swing angles, θ_u and θ_d were defined as indicated in Fig. 7. Subscripts of u and d denote upstream and downstream, respectively in the direction of rotating electromagnetic field. The swing angle with positive value indicates the arc is located at upstream side. On the other hand, the angle with negative value indicates the arc is at downstream side.

Figure 8 shows the time variation of arc swing angles at 12-phase during one AC period. The electrode was in the cathodic period during first half period, while that was in the anodic period during second half period. The arc swing angle during anodic period completely followed to the

rotation of electromagnetic field. On the other hand, the arc swing during the cathodic period has time delay from the rotation of electromagnetic field. The difference can be explained by the relationship between Lorentz force acting on the arc and inertial force due to electrode jet. Stronger cathode jet flow than anode jet flow leads to stronger inertial force, resulting in the time delay of the arc swing.

Figure 9 shows the time variation of arc swing angles at double 6-phase during one AC period. Differences of arc swing characteristics were observed between two same phase electrodes of double 6-phase. The arc of upstream electrode of rotating electromagnetic field often exists its

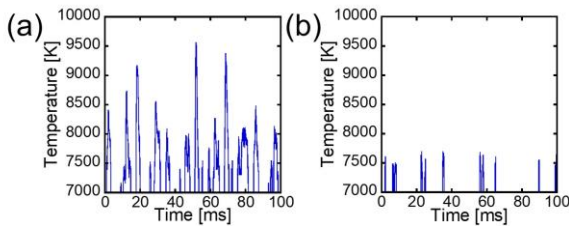


Fig. 5. Temperature fluctuation at the centre of the discharge region at 12-phase (a) and double 6-phase (b).

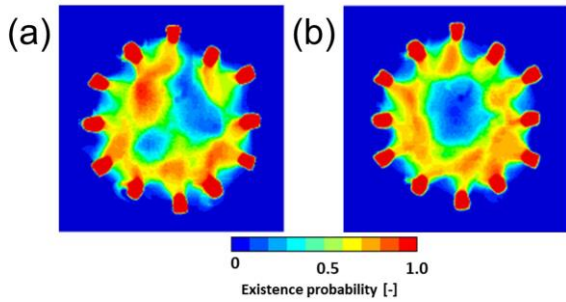


Fig. 6. Arc existence probabilities at 12-phase (a) and double 6-phase (b).

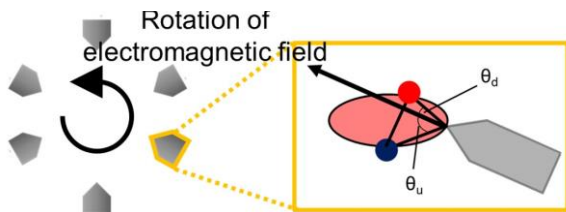


Fig. 7. Schematic diagram of analysis of arc swing

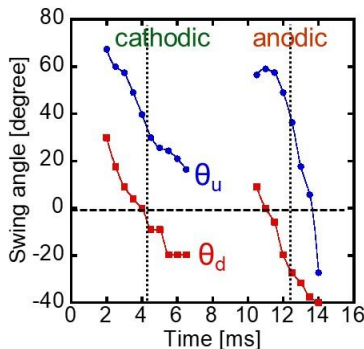


Fig. 8. Swing angle of arc during one AC cycle at 12-phase.

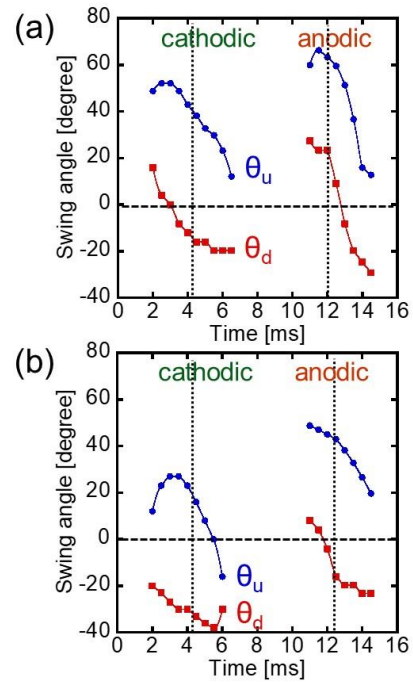


Fig. 9. Swing angle of arc during one AC cycle of upstream electrode at 2x6-phase (a) and downstream electrode at double 6-phase (b).

right side due to nearer electrode distance and larger phase shift of 60 degree. In contrast, the arc of downstream electrode of rotating electromagnetic field exists its right side because this electrode only follows the upstream electrode.

5. Conclusion

Arc fluctuation phenomena and temperature fluctuation characteristics of multiphase AC arc were successfully visualized by the high-speed camera and band-pass filters. Arc temperature of multiphase AC arc was fluctuated from 7000 K to 13000 K. This shows that the refractory metals or ceramics can be completely treated in the multiphase AC arc. AC applied condition of double 6-phase made the arc region in the outer circumference. Arc swing angle between cathodic and anodic period was clarified. Also, the difference of arc swing between 12-phase and 2x6-phase is visualized. Understanding the arc fluctuation phenomena and temperature fluctuation characteristic in the multiphase AC arc enables us to apply this to the various material processing at high productivity compared to the other thermal plasmas.

6. References

- [1] J. Heberlein, et al., *Journal of Physics D*, **43**, 2 (2010).
- [2] Y. Liu, et al., *J. Chem. Eng. Jpn.*, **46**, 672-676 (2013).
- [3] R. H. Fowler, et al., *Monthly Notices of the Royal Astronomical Society*, **83**, 403-424 (1923).
- [4] K. Hiraoka, et al., *Welding International*, **11**, 9 (1997).
- [5] S. Semenov, et al., *The European Physical Journal D*, **10**, 2 (2001).
- [6] B. Bachmann et al., *Journal of Physics D*, **46**, 12 (2013).